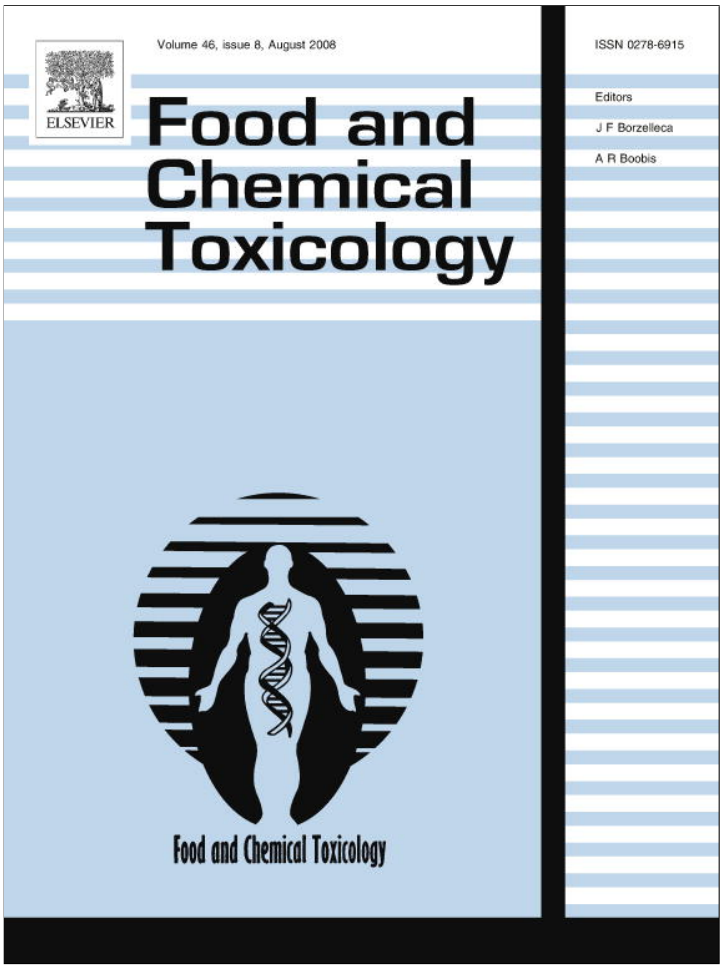

Food and Chemical Toxicology 46 (2008) 2694–2702

Contents lists available at ScienceDirect

Food and Chemical Toxicology

journal homepage: www.elsevier.com/locate/foodchemtox

(−)-Anonaine induces apoptosis through Bax- and caspase-dependent pathways in human cervical cancer (HeLa) cells

Chung-Yi Chen [a,1], Tsan-Zon Liu [b,1], Wei-Chang Tseng [c], Fung-Jou Lu [d], Ray-Ping Hung [c], Chi-Hung Chen [e], Ching-Hsein Chen [f,*]

[a] School of Medicine and Health Sciences, Fooyin University, Kaohsiung Hsien 831, Taiwan
[b] Center for Gerontological Research and Graduate Institute of Medical Biotechnology, Chang Gung University, Kwei-Shan, Taoyuan 333, Taiwan
[c] Department of Medical Technology, Fooyin University, Ta-Liao, Kaohsiung Hsien 831, Taiwan
[d] Department of Applied Chemistry, Chung Shan Medical University, Taichung 402, Taiwan
[e] Graduate Institute of Food Science and Biopharmaceutics, National Chiayi University, 300 University Road, Chiayi 60004, Taiwan
[f] Graduate Institute of Biomedical and Biopharmaceutical Sciences, College of Life Sciences, National Chiayi University, 300 University Road, Chiayi 60004, Taiwan

ARTICLE INFO

Article history:
Received 29 December 2007
Accepted 22 April 2008

Keywords:
(−)-Anonaine
Cervical cancer
Bax
Caspases
Apoptosis

ABSTRACT

(−)-Anonaine has been shown to have some anticancer activities, but the mechanisms of (−)-anonaine inducing cell death of human cancer cells is not fully understood. We investigated the mechanisms of apoptosis induced by (−)-anonaine in human HeLa cancer cells. Treatment with (−)-anonaine induces dose-dependent DNA damage that is correlated with increased intracellular nitric oxide, reactive oxygen species, glutathione depletion, disruptive mitochondrial transmembrane potential, activation of caspase 3, 7, 8, and 9, and poly ADP ribose polymerase cleavage. Our data indicate that (−)-anonaine up-regulated the expression of Bax and p53 proteins in HeLa cancer cells. The apoptosis and expression of Bax induced by (−)-anonaine could be inhibited when the HeLa cells were pretreated with Boc-Asp(OMe)-fmk, which is a broad caspases inhibitor. There was no obvious DNA damage in the (−)-anonaine-treated Madin–Darby canine kidney and Vero cell lines. Both Madin–Darby canine kidney and Vero cell lines are kidney epithelial cellular morphology. These results suggest that (−)-anonaine might be considered a potent compound for chemotherapy against cervical cancer or a health food supplement for cancer chemoprevention.

1. Introduction

Michelia alba D.C. (Magnoliaceae) is a tall tree native to Indonesia and has been used in Malaysians and Indonesia for medicinal purposes. The bark is used for the treatment of fever, syphilis, gonorrhea, and malaria; whereas, the white fragrant flower is used traditionally as an abortive agent (Asaruddin et al., 2003). (−)-Anonaine (Fig. 1), an alkaloid compound, is extracted from the leaves of *Michelia alba*. Several studies demonstrated that (−)-anonaine provided some biological and pharmacological activities, including vasorelaxant, antibacterial, antifungal, antioxidative, and antidepressant effects (Villar et al., 1987; Tsai et al., 1989; Martinez et al., 1992; Paulo et al., 1992; Ubeda et al., 1993; Chulia et al., 1995; Protais et al., 1995; Valiente et al., 2004). However, the anticancer effect of (−)-anonaine has not been extensively studied.

Cervical cancer, a slow growing squamous cell carcinoma, is a common disease in women. The mortality rate of cervical cancer is high even though the percentage of cure is nearly 100%. For example, the mortality of cervical cancer was about 37% in the United States in 2006. The clinical therapy of cervical cancer includes surgery, radiotherapy, and chemotherapy. For example, cisplatin is a common chemotherapeutic compound for cervical cancer. However, patients often develop resistance to cisplatin at the later stages of therapy. It seems necessary to develop new drugs to complement the present chemotherapeutic strategies.

In this study, we attempt to unravel the anticancer effects and mechanisms of (−)-anonaine against human cervical HeLa cancer cells. Several apoptotic events, such as generation of reactive oxygen species (ROS), nitric oxide (NO) production, glutathione (GSH) depletion, mitochondrial transmembrane potential dysfunction, activation of caspases, and expression of apoptosis-related proteins are addressed in this study.

Abbreviations: NO, nitric oxide; ROS, reactive oxygen species; NAC, *N*-acetylcysteine; GSH, glutathione; DAF-2, 4,5-diaminofluorescein; PI, propidium iodide; DMEM, Dulbecco's modified Eagle's medium; FBS, fetal bovine serum; $\Delta\Psi_m$, mitochondrial transmembrane potential; MDCK, Madin–Darby canine kidney.

* Corresponding author. Tel.: +886 5 2717837; fax: +886 5 2717778.
E-mail address: chench@mail.ncyu.edu.tw (C.-H. Chen).

[1] Both authors contribute equally.

0278-6915/$ - see front matter © 2008 Elsevier Ltd. All rights reserved.
doi:10.1016/j.fct.2008.04.024

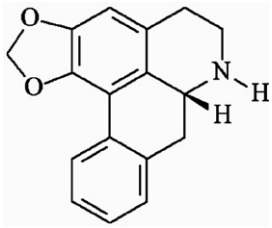

Fig. 1. The structure of (−)-anonaine.

2. Materials and methods

2.1. Plant material

The leaves of *M. alba* were collected from Fooyin University, Kaohsiung County, Taiwan in March, 2005. A voucher specimen (Michelia 2) was characterized by Dr. Yen-Ray Hsui of the Division of Silviculture, Taiwan Forestry Research Institute, Taipei, Taiwan, and deposited in the Basic Medical Science Education Center, Fooyin University, Kaohsiung County, Taiwan.

2.2. Plant experimental technology

Optical rotations were measured with a JASCO DIP-370 digital polarimeter. UV spectra were obtained in MeCN using a JASCO V-530 spectrophotometer. The IR spectra were measured on a Hitachi 260-30 spectrophotometer. ^1H (400 MHz, using $CDCl_3$ as solvent for measurement), ^{13}C (100 MHz), DEPT, HETCOR, COSY, NOESY, and HMBC NMR spectra were obtained on a Unity Plus Varian NMR spectrometer. LRFABMS and LREIMS were obtained with a JEOL JMS-SX/SX 102A mass spectrometer or a Quattro GC–MS spectrometer with a direct inlet system. Silica gel 60 (Merck, 230–400 mesh) was used for column chromatography. Precoated silica gel plates (Merck, Kieselgel 60 F-254, 0.20 mm) were used for analytical TLC, and precoated silica gel plates (Merck, Kieselgel 60 F-254, 0.50 mm) were used for preparative TLC. Spots were detected by spraying with 50% H_2SO_4 and then heating on a hot plate.

2.3. Extraction and isolation

The air-dried leaves of *M. alba* (6.0 kg) were extracted with MeOH (70 L × 6) at room temperature and a MeOH extract (367.8 g) was obtained upon concentration under reduced pressure. The MeOH extract, suspended in H_2O (1 L), was partitioned with $CHCl_3$ (2 L × 5) to give fractions soluble in $CHCl_3$ (154.3 g) and H_2O (144.1 g). The $CHCl_3$-soluble fraction was chromatographed over silica gel (800 g, 70–230 mesh) using *n*-hexane/$CHCl_3$/MeOH mixtures as eluents to produce five fractions. Part of fraction 4 (38.54 g) was subjected to silica gel chromatography by eluting with $CHCl_3$–MeOH (40:1), enriched with MeOH to furnish five fractions (4-1–4-5). Fraction 4-3 (15.12 g) was subjected to further silica gel chromatography eluted with $CHCl_3$–MeOH (50:1) and enriched gradually with MeOH. Three fractions were obtained (4-3-1–4-3-3). Fraction 4-3-3 (7.75 g), eluted with $CHCl_3$–MeOH (40:1), was further separated using silica gel column chromatography and gave (−)-anonaine (46 mg). (−)-Anonaine was identified by NMR data and confirmed by direct comparison with authentic samples from *Michelia compressa* (Lo et al., 2004). The purity of (−)-anonaine was >90% as determined by HPLC.

2.4. Cell lines and reagents

HeLa, Madin–Darby canine kidney (MDCK), and Vero cell lines were obtained from the American Type Culture Collection (Rockville, MD). THP-1, A549, U87MG, and SW480 cell lines were obtained from the Bioresource Collection and Research Center (Hsinchu, Taiwan, ROC). The "Apo-BrdU" kits were obtained from BD Pharmingen (San Diego, CA). The Apo-one™ homogeneous caspase 3/7 assay kit was purchased from Promega (Madison, WI). The caspase 8 and caspase 9 assay kits, FITC-IETD-FMK and FITC-LEHD-FMK were bought from United States Biological (Swampscott, Massachusetts). The anti-Bcl-2, anti-Bax, anti-p53, anti-actin and anti-PARP antibodies were obtained form Santa Cruz Biotechnology, Inc. (Santa Cruz, CA). Fetal bovine serum (FBS) was bought from Hyclone Co. (South Logan, UT) *N*-acetylcysteine (NAC), cyclosporin A, dexsamethasone, propidium iodide (PI), rhodamine123, 2′,7′-dichlorodihydrofluorescein-diacetate (DCFH-DA), 4,5-diaminofluorescein (DAF-2), Boc-Asp(OMe)-fmk, Dulbecco's modified Eagle's medium (DMEM), and other chemicals were purchased from Sigma Chemical Co. (St. Louis, MO).

2.5. Cell culture and treatment

The basal medium for cell culture was DMEM supplemented with 10% fetal bovine serum (FBS), 100 units/ml penicillin G, and 100 μg/ml streptomycin. The stock solution of (−)-anonaine was dissolved in DMSO, and different concentrations (μM) were prepared in the DMEM medium. The final DMSO concentration was less than 0.1%.

2.6. Cell cycle analysis of cancer and non-cancer cells

Cells were cultured in 60-mm tissue-culture dishes (8×10^5 cells/dish). The culture medium was replaced with a new DMEM medium after 24 h and then it was exposed to various concentrations of (−)-anonaine for 24 h. After treatment with (−)-anonaine, adherent and floating cells were pooled, washed with PBS, then fixed in PBS-methanol (1:2, volume/volume) solution, and finally maintained at 4 °C for at least 18 h. Following two more washes with PBS, the cell pellets were stained with the propidium iodide (PI) fluorescent probe solution containing PBS, 40 μg/ml PI, and 40 μg/ml DNase-free RNase A for 30 min at room temperature in the dark. DNA fluorescence of PI-stained cells was evaluated by excitation at 488 nm and monitored through a 630/22-nm band pass filter using a Becton–Dickinson FACS-Calibur flow cytometry (Franklin Lakes, NJ). A minimum of 10,000 cells were analyzed per sample, and the DNA histograms were gated and analyzed further using Modfit software on a Mac workstation to estimate the percentages of cells in various phases of the cell cycle.

2.7. Measurement of cell viability by MTT assay

Cell viability was determined by MTT assay. Cells (5×10^8) were cultured in 60-mm tissue-culture dishes for 24 h. The culture medium was replaced with new DMEM medium and then exposed to 100 μM of (−)-anonaine for 24 h. After treatments, cells were incubated for 2 h with 0.5 mg/ml of MTT reagent, lysed with DMSO. The absorbance was measured at 595 nm in a microplate reader (Bio-Rad, Richmond, CA).

2.8. Measurement of intracellular ROS by flow cytometry

Production of intracellular ROS was detected by flow cytometry using DCFH-DA (Chen et al., 2007). HeLa cells were cultured in 60-mm tissue-culture dishes. The culture medium was replaced with new medium when the cells were 80% confluent and then exposed to 100 μM of (−)-anonaine for 1, 3, and 24 h. After treatment, cells were treated with 10 μM DCFH-DA for 30 min in the dark, washed once with PBS, detached by trypsinization, collected by centrifugation, and suspended in PBS. The intracellular ROS as indicated by the fluorescence of dichlorofluorescein (DCF) was measured with a Becton–Dickinson FACS-Calibur flow cytometer.

2.9. Measurement of intracellular NO by flow cytometry

Production of intracellular NO was detected by flow cytometry using DAF-2 (Hsieh et al., 2005). HeLa cells were cultured in 60-mm tissue-culture dishes. The culture medium was replaced with new medium when the cells were 80% confluent and then exposed to 100 μM of (−)-anonaine for 1, 3, and 24 h. After treatment, cells were treated with 1 μM DAF-2 for 10 min in the dark, washed once with PBS, detached by trypsinization, collected by centrifugation, and suspended in PBS. The DAF-2 fluorescence reflecting the level of intracellular NO in cells was measured in a Becton–Dickinson FACS-Calibur flow cytometer.

2.10. Measurement of GSH depletion by flow cytometry

Cells (8×10^5) were cultured in 60-mm tissue-culture dishes for 24 h. The culture medium was replaced with new medium when the cells were 80% confluent and then exposed to 100 μM of (−)-anonaine for 1, 3, 6, 9, 12, and 24 h. After treatment, the cells were incubated with 25 μM CMF-DA for 20 min at 37 °C in the CO_2 incubator. The CMF fluorescence is directly related to intracellular GSH level. After CMF-DA staining, the cells were washed with PBS, collected by centrifugation, then measured with a Becton–Dickinson FACS-Calibur flow cytometer (Chen et al., 2007).

2.11. Measurement of $\Delta\Psi_m$ by flow cytometry

Rhodamine123 is a fluorescent dye that is incorporated into mitochondria in a $\Delta\Psi_m$-dependent manner (Chen et al., 2007). HeLa cells were cultured in 60-mm tissue-culture dishes. The culture medium was replaced with new medium when the cells were 80% confluent and then exposed to 100 μM of (−)-anonaine for 3, 6, 9, 12, and 24 h. After treatment, the culture medium was replaced with a new medium with 5 μM rhodamine123 for 30 min in the dark. Subsequent to the incubation step, cells were harvested by trypsinization, following which, $\Delta\Psi_m$ as indicated by the fluorescence level of rhodamine123, was analyzed using a Becton–Dickinson FACS-Calibur flow cytometer.

2.12. Measurement of caspase 3, 7, 8, and 9 activities by flow cytometry

Caspase 3, 7, 8, and 9 activities were measured by a method modified from an experienced user's protocol on Apo-one™ homogeneous caspase 3/7 assay kit. The caspase substrates, Z-DEVD-R110 for caspase 3/7, FITC-IETD-FMK for caspase 8, and FITC-LEHD-FMK for caspase 9, were diluted with a buffer to make the desired amount of various homogeneous substrate reagents. HeLa cells were cultured in 60-mm tissue-culture dishes. The culture medium was replaced with a new medium when the cells were 80% confluent and then treated with 100 μM (−)-anonaine

for 3, 6, 9, 12, and 24 h. After treatment, the cells were washed once with PBS, detached by trypsinization, and collected by centrifugation. Aliquot 8×10^5 cells were suspended in a DMEM medium, then various homogeneous substrate reagents were added to the cells, maintaining a 1:1 ratio of reagent to cell solution. After 1 h of incubation at 37 °C, the cells were washed once with PBS, collected by centrifugation, and suspended in PBS. Substrate cleavage to release free R110 or FITC fluorescence intensities were measured in a Becton–Dickinson FACS-Calibur flow cytometer with excitation wavelength set at 488 nm and emission wavelength at 520 nm.

2.13. Measurement of Bax, Bcl-2, and p53 and the cleavage of poly ADP ribose polymerase (PARP) by Western blotting

HeLa cells (8×10^5) were cultured in 60-mm tissue-culture dishes for 24 h. The culture medium was replaced with new medium and then exposed to 100 μM (−)-anonaine for 3, 6, 9, 12 and 24 h. After treatment, cells were washed with PBS, resuspended in protein extracted buffer for 10 min and then centrifuged at 12,000g for 10 min at 4 °C to obtain total extracted proteins (supernatant). The protein concentrations were measured with a Bio-Rad protein assay reagent (Bio-Rad, Richmond, CA) containing Coomassie Brilliant Blue G-250 dye. It is a dye-binding assay in which a differential color change of a dye occurs in response to various concentrations of protein. The absorbance maximum for an acidic solution of Coomassie Brilliant Blue G-250 dye shifts from 465 nm to 595 nm when binding to protein occurs. The Bax, Bcl-2, p53, PARP and actin expression were evaluated by Western blotting analysis. Briefly, the total extracted proteins were boiled in loading buffer, and an aliquot corresponding to 50 μg of protein was separated by 12% SDS-polyacrylamide gel. After electrophoresis, proteins were electrotransferred onto a polyvinylidene fluoride (PVDF) transfer membrane. After blotting, the membranes were incubated with anti-Bax, anti-Bcl-2, anti-p53, anti-PARP and anti-actin antibodies (Lab Vision and Santa Cruz, CA) overnight, then washed with PBST solution (0.05% Tween 20 in PBS). Following washing, the second antibody labeled with horseradish-peroxidase was adjacently incubated for 1 h, then washed with PBST solution (0.05% Tween 20 in PBS). The antigen–antibody complexes were detected by the enhanced chemiluminescence (Amersham Pharmacia Biotech, Piscataway, NJ) with a chemiluminescence analyzer.

2.14. TUNEL assay for apoptosis

Following incubation of various compounds, TUNEL was performed with the "Apo-BrdU" kits (BD Pharmingen, San Diego, CA), with the standard protocol provided by the manufacturer being used. Both floating and adherent cells were harvested and fixed using 1% paraformaldehyde for 20 min at 4 °C. After fixation, cells were permeated with 70% ethanol for 30 min at 4 °C. To label DNA strand breaks, 8×10^5 cells were incubated with 50 μl of TUNEL reaction buffer containing terminal deoxynucleotidyl transferase and BrdUTP for 1 h, and it was then incubated with FITC conjugated BrdUTP-antibody for 30 min at 37 °C in a humidified 5% CO_2-in-air atmosphere. Cells were washed twice with PBS, suspended in PBS containing 50 μg/ml of PI and 50 μg/ml of DNase-free RNase A for 30 min at room temperature in the dark and then analyzed by a Becton–Dickinson FACS-Calibur flow cytometer.

2.15. Statistical analysis

Data were presented as means ± standard errors from at least three independent experiments and analyzed using Student's *t* test. A *P* value of less than 0.05 was considered as statistically significant (Lucke, 1996).

3. Results

3.1. (−)-Anonaine induced DNA damage and decreased cell viability in various cancer cells but not in MDCK and Vero cells

To evaluate the effect of (−)-anonaine on DNA damage, the HeLa cells were treated with (−)-anonaine at 0, 25, 50, and 100 μM concentrations for 24 h. The percentages of various phases in cell cycle were evaluated by propidium iodide staining and flow cytometry. In Fig. 2, the SubG1 represents as DNA-damaged fragments. As shown in Fig. 2A, untreated cells expressed 50.7% of G1, 25.9% of S, 23.9% of G2/M, and 0.8% of SubG1. The percentage of SubG1 increased to 2.2% and 27% in 25 and 50 μM of (−)-anonaine-treated cells, respectively. The DNA damage increased markedly at 100 μM of (−)-anonaine treatment, and the percentage of SubG1 was 40.8% (Fig. 2A). The effect of DNA damage in (−)-anonaine treatment was also evaluated using two non-cancer cell lines, MDCK and Vero cells. As shown in Fig. 2B, 100 μM of (−)-anonaine treatment could not induce a significant increase of the percentage of SubG1 (<10%).

The DNA damage of (−)-anonaine treatment on other cancer cell lines was evaluated by flow cytometry. In Fig. 2C, the results showed that 100 μM of (−)-anonaine induced marked DNA damage to human acute monocytic leukemia THP-1 cells (35.3% of Sub G1) and slight damage to human lung cancer A549 and colorectal cancer SW480 cell lines by 19.0% and 11.6% of Sub G1, respectively. However, the (−)-anonaine-induced DNA damage was not apparent in human glioma U87MG cells (2.7% of Sub G1).

To evaluate the cell viability, the MTT assay was used. As shown in Fig. 2D, the cell viability of (−)-anonaine-treated HeLa cells decreased to 23 ± 1%. However, the cell viabilities in (−)-anonaine-treated Vero and MDCK cells were 75 ± 3% and 95 ± 4%, respectively. (−)-Anonaine inhibited the viability of HeLa cancer cells more effectively then the non-cancer cells.

3.2. (−)-Anonaine induced ROS and NO formations in HeLa cells

Many anticancer compounds induce apoptosis in cancer cells through an increased intracellular ROS content. The treatment of (−)-anonaine (100 μM) in HeLa cells resulted in a burst of ROS and the ROS formation reached the maximum after 1 h (Fig. 3A) as measured by DCF fluorescence (220 ± 19). The DCF fluorescence intensity increased significantly to 191 ± 21 and 162 ± 16 after 3 and 24 h of (−)-anonaine treatment, respectively. The DCF fluorescence declining with time might indicate that some ROS generated systems such as electron transport chain or NADPH oxidase were destroyed by (−)-anonaine treatment in mitochondrial or cellular membranes. In addition, the (−)-anonaine-treated cells might synthesize GSH to scavenge intracellular ROS, therefore, DCF fluorescence declined.

Several studies demonstrated that the NO expressed anti-tumor activity. High concentrations of NO can inhibit cell growth and induce apoptosis. The effect of (−)-anonaine (100 μM) on the production of intracellular NO in HeLa cells was evaluated by DAF-2 probe and flow cytometry. Results showed that (−)-anonaine significantly increased the DAF-2 fluorescence to 179 ± 14 after 3 h treatment, as compared with untreated cells (108 ± 6) (Fig. 3B). The maximal DAF-2 fluorescence (300 ± 19) was observed after 24 h of treatment (Fig. 3B).

3.3. (−)-Anonaine induced GSH depletion in HeLa cells

Intracellular GSH is important for defending against exogenous damage of anticancer compounds in many cancer cells. Once intracellular GSH depletion has occurred, the cells proceed to apoptosis. Because (−)-anonaine (100 μM) induced a large amount of ROS in HeLa cells, the levels of intracellular GSH depletion by (−)-anonaine were evaluated at various time points. In Fig. 3C, the GSH depletion was not obvious after up to 12 h of treatment, in which the cellular percentage of GSH depletion was less than 10%. The cellular percentage of GSH depletion significantly increased to 78% after 24 h of treatment as compared with untreated cells. In Fig. 3D, the percentages of GSH depletion in (−)-anonaine-treated Vero and MDCK cells were 3.5 and 3.9, respectively. These data suggested that the (−)-anonaine could not induce GSH depletion in the normal cell lines.

3.4. (−)-Anonaine induced $\Delta\Psi_m$ to decrease in HeLa cells

The loss of mitochondrial membrane potential ($\Delta\Psi_m$) is an important event in apoptosis (Wang et al., 2006). The $\Delta\Psi_m$ was evaluated in (−)-anonaine-treated HeLa cells by using the rhodamine 123 fluorescent dye, which specifically accumulated within the mitochondrial compartment in a $\Delta\Psi_m$ dependent manner. As shown in Fig. 4A, the untreated cells expressed rhodamine 123 fluorescence between 508 and 528 relative fluorescent units. The rhodamine 123 fluorescence was significantly decreased after 3,

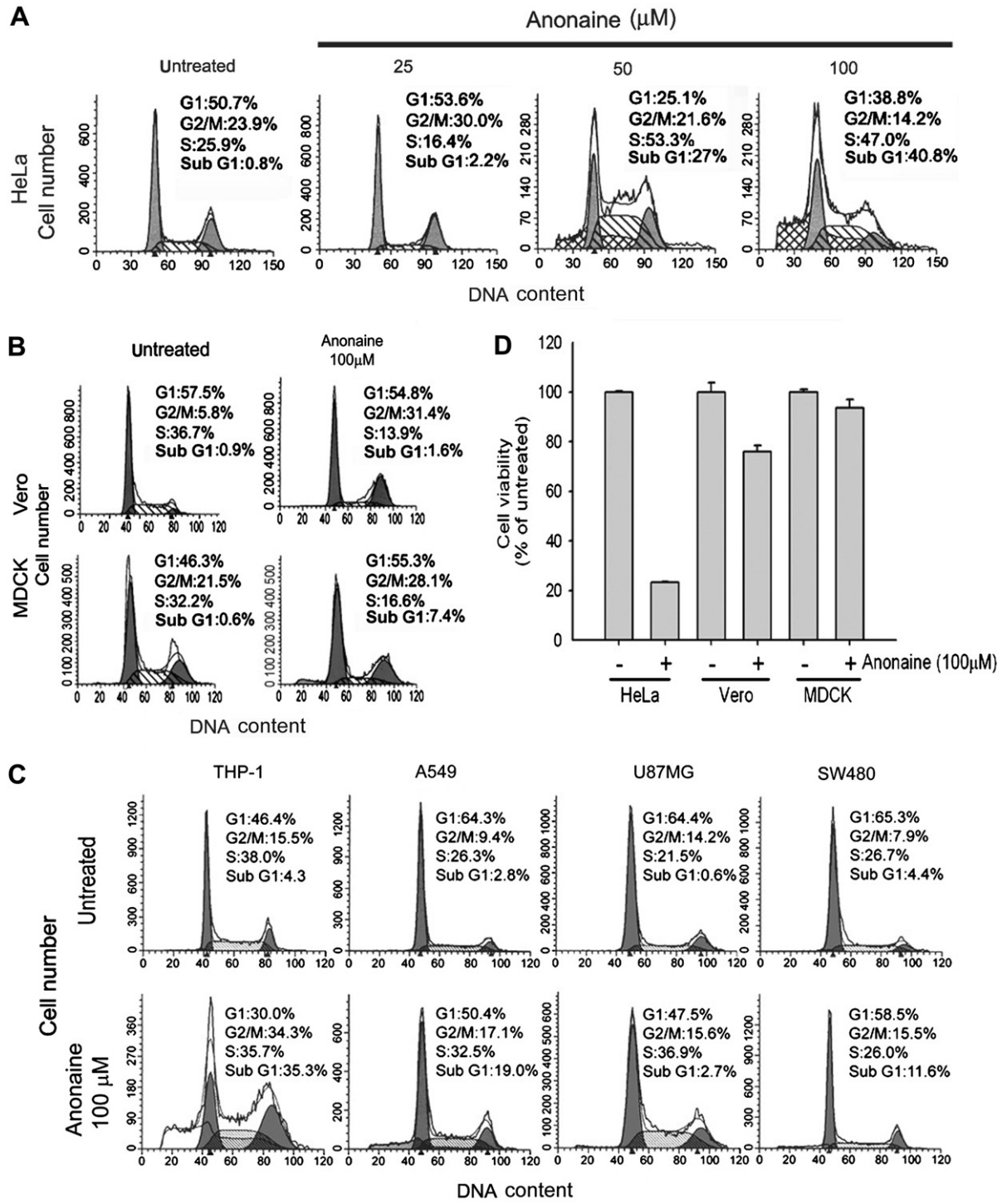

Fig. 2. Cell cycle and DNA damage analysis in (−)-anonaine-treated (A) HeLa, (B) Vero and MDCK (C) THP-1, A549, U87MG, and SW480 cell lines. After drugs treatment, adherent and floating cells were harvested and analyzed by flow cytometry. (D) Cell viability analysis in (−)-anonaine-treated HeLa, Vero and MDCK cell lines. These experiments were performed at least three times and a representative experiment is presented.

6, 9 and 12 h of treatment, respectively. The maximum loss of $\Delta\Psi_m$ was observed after 24 h of treatment.

3.5. Effect of caspase 3, 7, 8, and 9 activities in (−)-anonaine treated HeLa cells

To evaluate the role played by caspases in the apoptotic effect induced by (−)-anonaine in HeLa cells, the caspase 3, 7, 8, and 9 activities were examined after 3, 6, 9, 12 and 24 h of treatment. Fig. 4B shows that the activities of caspases 8 and 9 were time-dependently increased after (−)-anonaine treatment. Both activities of caspases 8 and 9 increased about 4-fold after 24 h of treatment. In particular, the activities of caspase 3/7 were enhanced significantly after (−)-anonaine treatment. The highest activity of caspase 3/7 induced by (−)-anonaine appeared after 12 h of treatment (1125 ± 13).

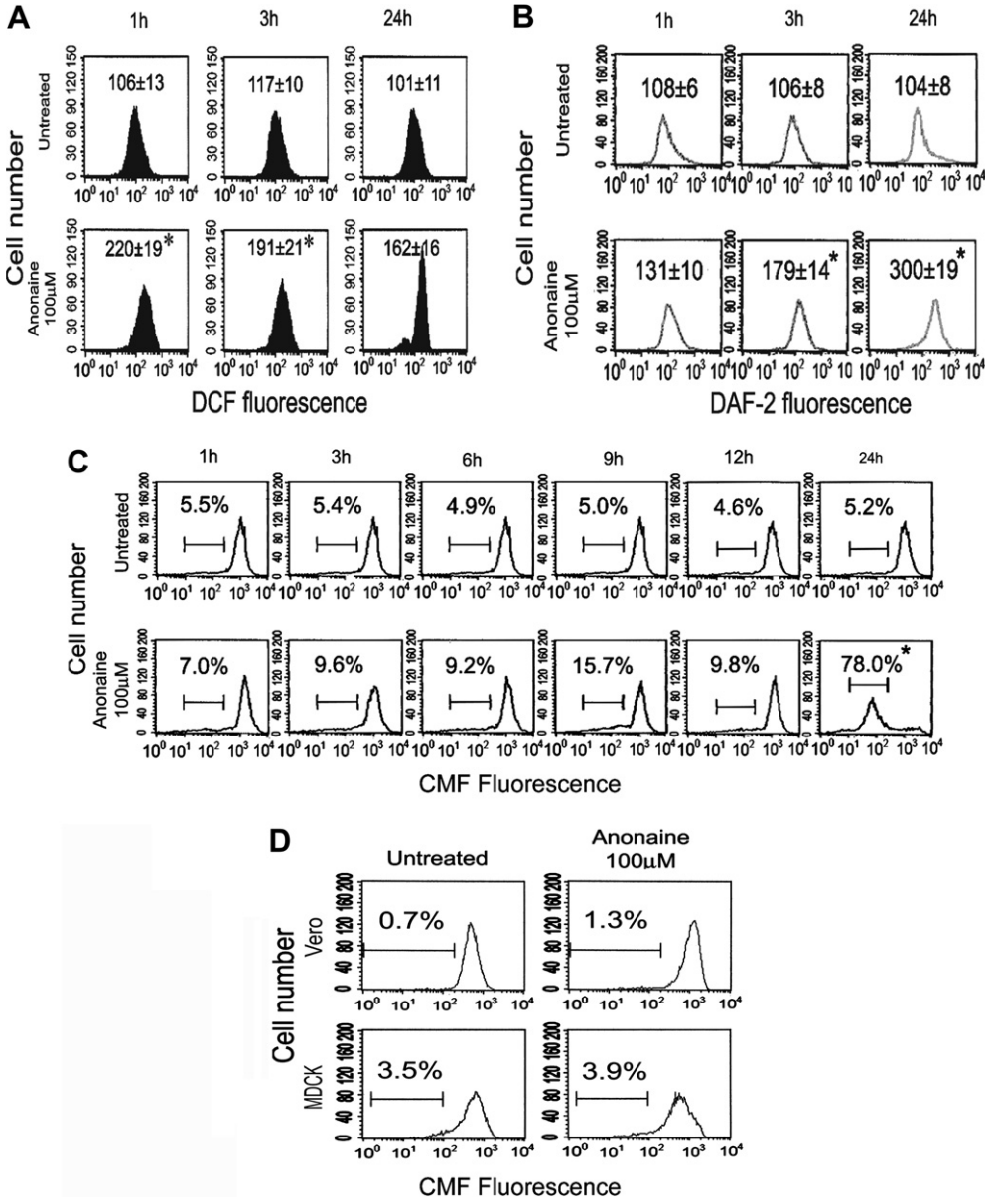

Fig. 3. Intracellular ROS, NO and GSH depletion analysis. After treatment, cells were treated with (A) 10 μM DCFH-DA for 30 min (B) 1 μM DAF-2 for 10 min. The fluorescence of dichlorofluorescein (DCF) and DAF-2 was measured with a Becton–Dickinson FACS-Calibur flow cytometer. The data in each panel represents the DCF or DAF-2 fluorescence intensity within the cells. The values shown are mean ± standard errors (n = 6 of individual experiments). Significant differences from the untreated group are $P < 0.05$ (*). (C) and (D) After treatment, the cells were incubated with 25 μM CMF-DA for 30 min, and then measured by flow cytometry. Data represent the percentage of cells displaying intracellular GSH negative cells. These experiments were performed at least three times and a representative experiment is presented.

3.6. The expression of Bax, Bcl-2, and p53 and the cleavage of poly ADP ribose polymerase (PARP) in (−)-anonaine-treated HeLa cells

Several apoptotic related proteins were evaluated in (−)-anonaine treated HeLa cells. As shown in Fig. 5, the expression of Bax increased time-dependently after (−)-anonaine treatment, and the maximal expression was after 24 h of treatment. The expression of Bcl-2 and p53 also increased time-dependently from 3 to 12 h of treatment and then decreased after 24 of treatment. The cleavage of PARP appeared markedly after 9, 12, and 24 h of (−)-anonaine treatment.

3.7. Evaluate critical pathway in (−)-anonaine-induced apoptosis

The intracellular ROS overproduction can activate caspase 3/7 activities and eventually provokes apoptosis (Jia and Misra, 2007). To further evaluate the effect of (−)-anonaine-induced ROS on caspase 3/7 activation, HeLa cells were pretreated by three antioxidants, 10 mM GSH, 10 mM *N*-acetylcysteine (NAC), and 100 μM vitamin C for 1 h and followed by treatment with 100 μM (−)-anonaine for another 9 h, and then analyzed the caspases 3/7 activities by flow cytometry. As shown in Fig. 6A, three antioxidants did not inhibit the activation of caspases 3/7 in (−)-anonaine-treated cells. The Bax-dependent apoptosis could result from the caspase 3 pathway (Achiwa et al., 2005; Altznauer et al., 2004). To evaluate whether Bax overexpression would directly depend on the caspases 3/7 activation by (−)-anonaine treatment, the HeLa cells were pretreated with Boc-Asp(OMe)-fmk (a broad caspases inhibitor) for 1 h, and then treated with (−)-anonaine for another 24 h. The Bax expression was analyzed by western blotting. In Fig. 6B, the Boc-Asp(OMe)-fmk treatment inhibited the Bax expression in (−)-anonaine-treated cells. To investigate

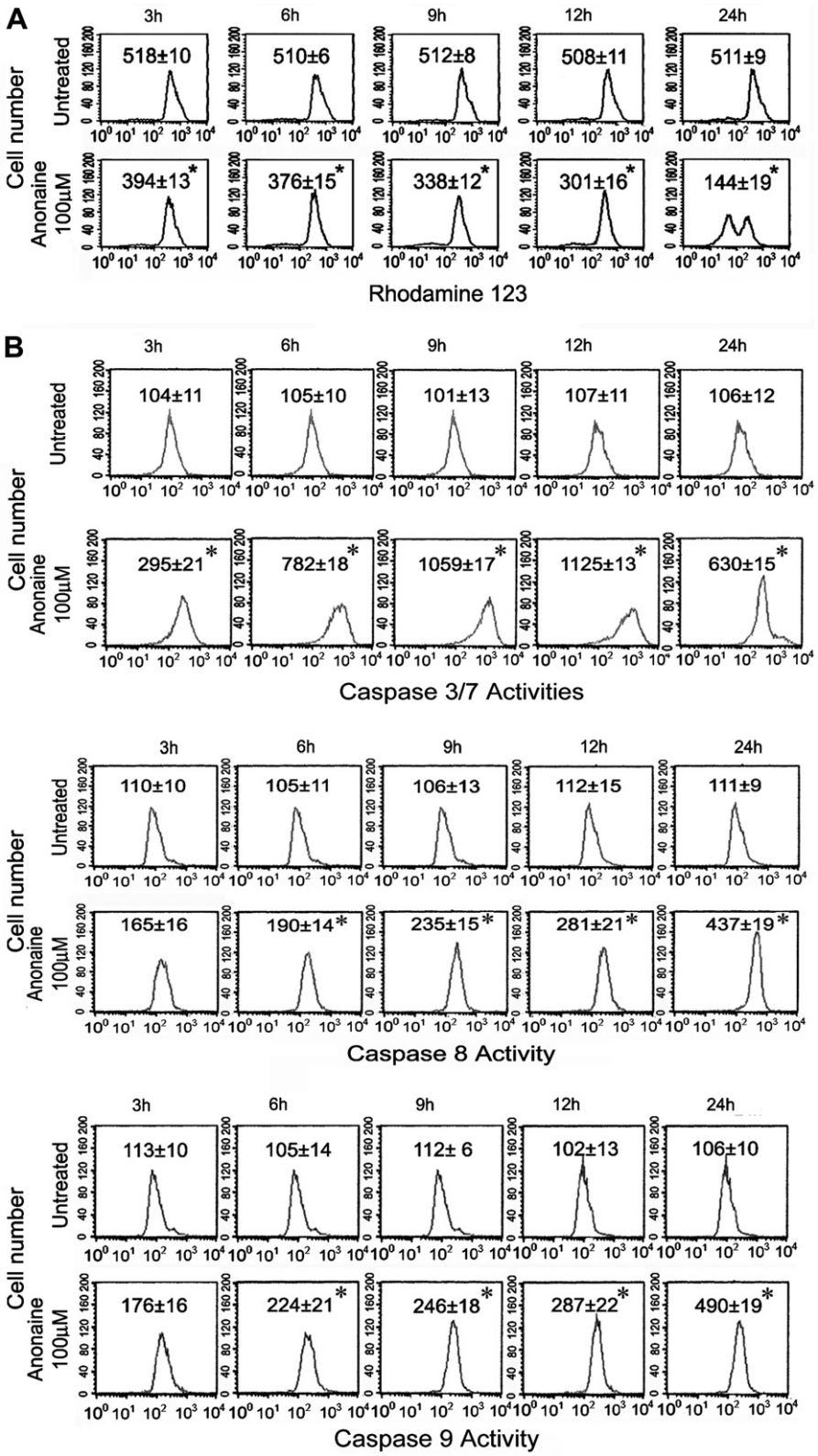

Fig. 4. Mitochondrial transmembrane potential ($\Delta\Psi_m$), caspase 3, 7, 8, and 9 activities analysis in (−)-anonaine-treated HeLa cells. (A) After treatment, the cells were incubated with 5 μM rhodamine for 30 min, and then measured by flow cytometry. Data represent the rhodamine 123 fluorescence intensity within the cells. (B) After treatment, cells were suspended in various homogeneous substrate reagents for 1 h at 37 °C, and then measured by flow cytometry. The data in each panel represents the fluorescence intensity within the cells. Values shown are mean ± standard deviation ($n = 6$). Significant differences from the untreated group are $P < 0.05$ (*).

the critical pathway on (−)-anonaine-induced apoptosis, the HeLa cells were pretreated by 100 μM Boc-Asp(OMe)-fmk, 10 mM NAC, 10 mM GSH, 1 mM mannitol, and 100 u/ml catalase (four antioxidants), 10 μM dexsamethasone (a NO inhibitor), 5 μM cyclosporin A (a mitochondrial permeability transition opening inhibitor), and 10 μM pifithrin-α (a p53 inhibitor) for 1 h and followed by

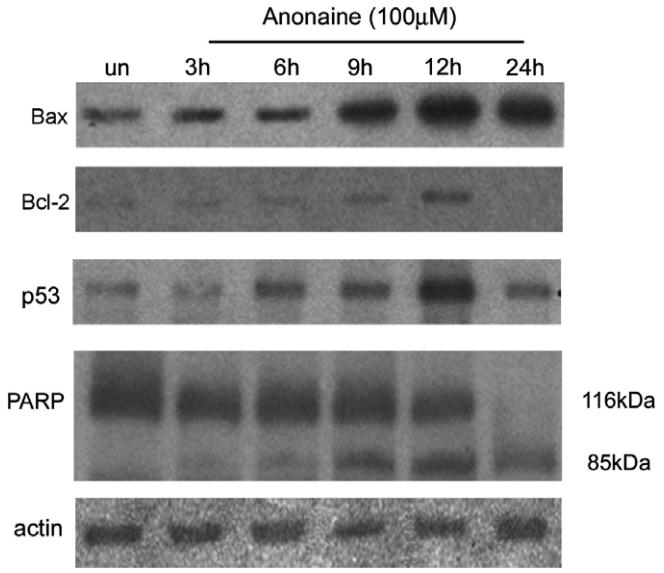

Fig. 5. Western blotting analysis in (−)-anonaine-treated HeLa cells. After treatment, cells were washed with PBS, extracted with protein extracted buffer. Fifty micrograms of proteins were loaded on a 12% SDS-polyacrylamide gel. The expressions of Bax, Bcl-2, p53, PARP and actin were evaluated by Western blotting analysis. These experiments were performed at least three times and a representative experiment is presented.

treatment with (−)-anonaine for another 9 h and then analyzed by TUNEL assay. As shown in Fig. 6C, the percentage of apoptotic cells in the untreated group was 0.3% and increased to 92% at 24 h in the 100 μM (−)-anonaine-treated cells. The percentage of apoptosis in Boc-Asp(OMe)-fmk-pretreated cells exhibited the lowest level (18%) after 24 h of treatment. The other pretreated compounds did not markedly decrease the percentages of apoptosis induced by (−)-anonaine.

4. Discussion

Recently, we have found several alkaloid compounds such as secokotomolide A, actiondaphnine, and 6-shogaol that could induce apoptosis through increasing intracellular ROS and GSH depletion at early and late periods of treatment, respectively, in some cancer cells (Hsieh et al., 2006; Chen et al.,2006, 2007). Apoptosis induced by the alkaloid compounds could be blocked by pretreatment with the antioxidants GSH or NAC. The ROS increase induced by anticancer compounds could induce apoptosis in many cancer cells. Many chemotherapeutic compounds obtained from plants such as berberine and kaempferol also induce large amounts of intracellular ROS to kill many types of cancer cells (Sharma et al., 2007; Syed et al., 2008). These results seem to explain the importance of the intracellular ROS overproduction by anticancer compounds. Although (−)-anonaine could induce ROS and NO formation during 24 h treatment, NAC, GSH, and mannitol (three antioxidants), catalase (a H_2O_2 scavenging enzyme), or dexamethasome (a NO inhibitor) were not effective in preventing the apoptotic effect of (−)-anonaine-treated in HeLa cells (Fig. 6C). NAC, an intracellular GSH supplement agent, could not prevent the apoptosis in (−)-anonaine-treated cells, which suggests that GSH depletion is not necessarily the critical event. The results were in contradiction to our previous findings in anticancer mechanisms of other alkaloid compounds (Chen et al., 2006, 2007; Hsieh et al., 2006). The (−)-anonaine-induced ROS overproduction and GSH depletion do not play an important role in the HeLa cells' apoptosis.

ROS overexpression could induce p53-Bax pathway and eventually result in apoptosis. For example, oxidized low-density lipoprotein could activate p53 through production of mitochondria-derived ROS. Under the treatment of NAC, the p53-Bax pathway activated by oxidized low-density lipoprotein was blocked, and apoptosis was prevented (Cheng et al., 2007). In our present studies, three antioxidants, NAC, GSH, and mannitol and one H_2O_2 scavenging enzyme, catalase, did not effectively inhibit the (−)-anonaine-induced apoptosis. Moreover, antioxidants, NAC, GSH, and vitamin C did not effectively inhibit the (−)-anonaine-induced caspase 3/7 activation. These results explain that the ROS-induced p53-Bax pathway is not the critical event in (−)-anonaine induced apoptosis but do affirm that ROS is an essential and necessary initial death signaling for (−)-anonaine-induced death through p53-Bax pathway.

The effects of some anticancer compounds are indeed mediated by low levels of Bcl-2 and Bcl-x(L) proteins (Mitsunaga et al., 2007). In our study, the expression of anti-apoptotic protein, Bcl-2, increased time-dependently from 3 to 12 h of (−)-anonaine treatment but disappeared after 24 h of treatment. The increase of Bcl-2 might indicate a drug-resistant effect in cancer cells. The overexpression of pro-apoptotic protein Bax and tumor suppressor protein p53 play an important event in anticancer compounds-induced apoptosis. For example, Bax and p53 could combine to form a Bax/p53 complex and then enter the nucleus and induce apoptosis in cisplatin treated cancer cells; at the same time the cytoplasmic apoptosis-related caspase 3 could be activated prior to the detection of apoptotic DNA fragmentation (Raffo et al., 2000). These findings are similar to our results. Four caspases (caspase 3, 7, 8, and 9) activation exhibited a time-dependent event during 3–12 h of (−)-anonaine treatment (Fig. 4B). The activity of caspase 3/7 could be induced to the highest level (10.5-fold) after 12 h of treatment. In the meantime, Bax, p53 and the PARP cleavage (85 kDa) were extensively overexpressed (Fig. 5).

It is of interest to note that Bax is a downstream transcriptional target of p53 (Chipuk et al., 2004). It explains that the p53 expression induced by (−)-anonaine might lead to the Bax overexpression. In spite of the expression of p53 has already disappeared, the Bax still overexpressed at 24 h. The p53 inhibitor, pifithrin-α could not prevent the apoptosis in (−)-anonaine-treated cells (Fig. 6C). The results explain that the overexpression of p53 alone could not effectively induce apoptosis; p53 might combine with Bax in order to induce apoptosis effectively in the (−)-anonaine-treated HeLa cells. In addition, Mitsunaga et al. (2007) showed that Bax and p53 were related to caspase-dependent apoptosis. In our study, the broad caspases inhibitor, Boc-Asp(OMe)-fmk inhibited the Bax expression and apoptosis in the (−)-anonaine treated cells. The p53 can directly activate the Bax expression and mediate mitochondrial membrane permeabilization and apoptosis (Chipuk et al., 2004). In Fig. 5, the p53 expression is increased to 12 h. The Bax expression is also increased to 12 h and might be related to the p53 expression in (−)-anonaine treatment. These results illustrate that the (−)-anonaine induced apoptosis is caspases- and Bax-dependent.

A rapid collapse of $\Delta\Psi_m$ is always found in some anticancer compounds-induced apoptosis in cancer cells (Chen et al., 2007, 2006; Wang et al., 2006; Hsieh et al., 2006). In the (−)-anonaine-treated HeLa cells, the $\Delta\Psi_m$ level maintains a moderate decrease after 3–12 h of treatment, but serious loss occurs after 24 h of treatment (Fig. 4A). Pretreated with cyclosporin A (a mitochondrial permeability transition opening inhibitor), the percentage of apoptosis only decreased from 92% to 85% (Fig. 6C). These results explain that $\Delta\Psi_m$ decrease is not a critical event in (−)-anonaine-induced apoptosis.

The purpose of this study is to evaluate the apoptosis and its pathway in (−)-anonaine-treated HeLa cells. In Fig. 2, 100 μM of

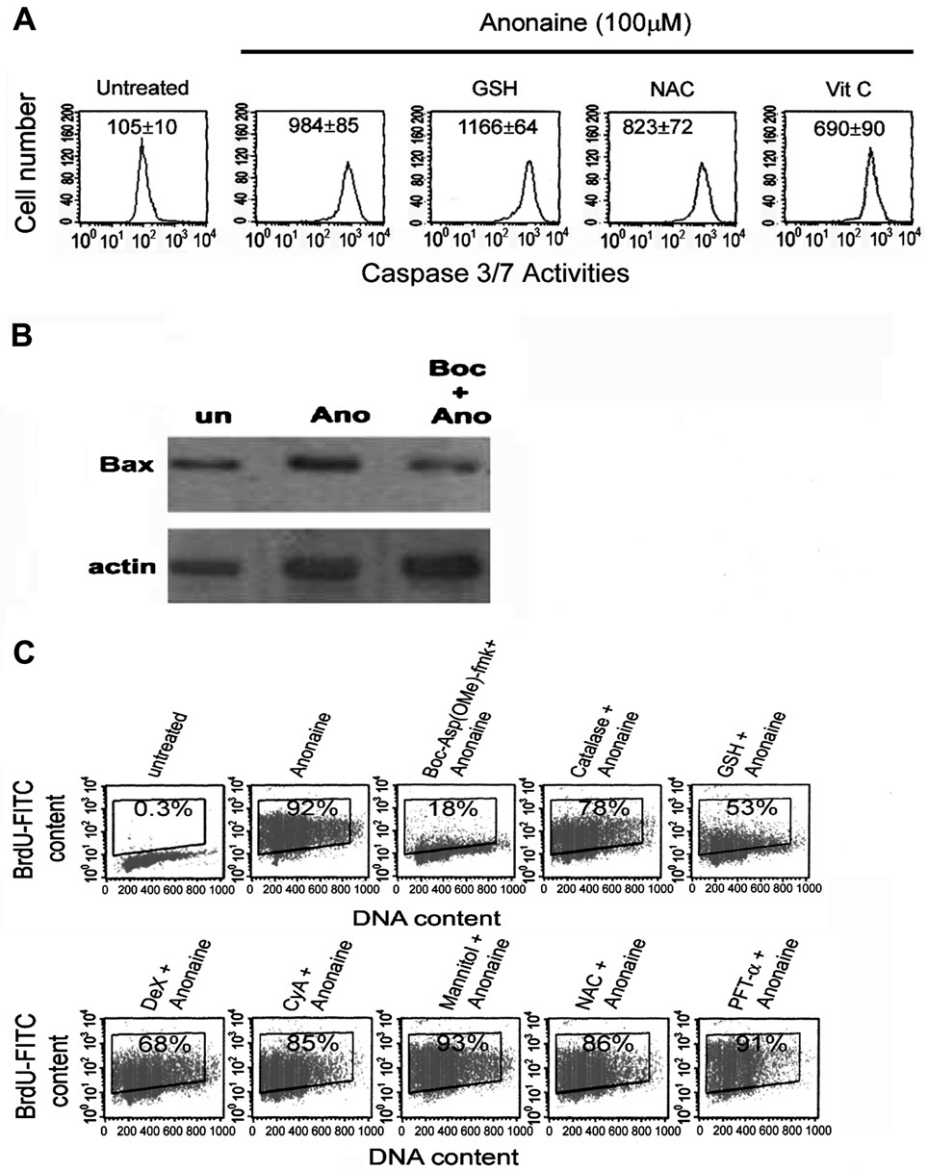

Fig. 6. Evaluation of critical role in (−)-anonaine-induced apoptosis. (A) The HeLa cells were treated with 0 (untreated) or 100 μM (−)-anonaine alone for 24 h, pretreated with 10 mM GSH, 10 mM NAC, or 100 μM vitamin V (Vit C) for 1 h, followed by 100 μM (−)-anonaine treatment for 9 h, and then analyzed the caspase 3/7 activities. (B) The HeLa cells were treated with 0 (untreated) or 100 μM (−)-anonaine (Ano) alone for 24 h, pretreated with 100 μM Boc-Asp(OMe)-fmk (Boc) for 1 h, followed by 100 μM (−)-anonaine (Ano) treatment for 24 h, and then analyzed the Bax expression by Western blotting. (C) The HeLa cells were treated with 0 (untreated) or 100 μM (−)-anonaine alone for 24 h, pretreated with 100 μM Boc-Asp(OMe)-fmk, 100 U/ml catalase, 10 mM GSH, 10 μM dexsamethasone (Dex), 5 μM cyclosporin A (CyA), 1 M mannitol, 10 mM NAC, or 10 μM pifithrin-α(PFT-α) for 1 h, followed by 100 μM (−)-anonaine treatment for 24 h, and then proceeded to the TUNEL assay. The representative plots depict DNA content on the *x*-axis and BrdU-FITC-labeled apoptotic DNA strand breaks on the *y*-axis. Data represent the percentage of cells in the upper box of apoptosis. These experiments were performed at least three times and a representative experiment is presented.

(−)-anonaine treatment in 40.8% of SubG1. Lower doses of (−)-anonaine at 25 and 50 μM did not induce a large percentage of SubG1 (less than 40%). To ensure the apoptosis induction by (−)-anonaine, we selected a high dose of (−)-anonaine (100 μM). Sanguinarine, a natural compound, was more effective to induce apoptosis as low as 5–10 μM doses in various cancer cell lines. The difference of the effective doses between sanguinarine and (−)-anonaine on apoptosis of cancer cells may be due to the difference of chemical structures of these two compounds and their DNA binding abilities.

It is worth to note that the DNA damage did not occur in (−)-anonaine-treated non-cancer cell lines, MDCK and Vero cells (Fig. 1B). The origin of Vero cells is African Green Monkey kidney cells. MDCK and Vero cells used for comparison with HeLa cells for three reasons: Firstly, the kidney is an important organ for excreting various toxic substances and drugs. Both MDCK and Vero cells are kidney cellular types. To evaluate whether (−)-anonaine-induced DNA damage in kidney cellular types, both MDCK and Vero cells were used in this study. Secondly, HeLa cells as well as MDCK and Vero cells belong to epithelial cellular morphology. On the same cellular morphology, we compared the (−)-anonaine-induced DNA damage in HeLa cancer cells and two MDCK and Vero non-cancer cells. Thirdly, a potent anticancer compound for chemoprevention or chemotherapy should be non-toxic to normal cells but toxic to various cancer cells. We tested the DNA damage in two MDCK and Vero non-cancer cells. If (−)-anonaine induce low level of DNA damage in two MDCK and Vero non-cancer cells, it might increase the worth of (−)-anonaine in anticancer effect. (−)-Anonaine

seems to fall into this category i.e. killing specific cancer cells, but safe to normal cells. Nevertheless, further research on the effectiveness (−)-anonaine treatment of different cancer cells is still necessary.

Conflict of interest statement

The authors declare that there are no conflicts of interest.

Acknowledgements

This work was supported by Grant NSC 95-2320-B-415-005 (C.-H. Chen) and NSC 95-2320-B-242-004 (C.-Y. Chen) from the National Science Council, Taiwan, ROC.

References

Achiwa, Y., Hasegawa, K., Komiya, T., Udagawa, Y., 2005. Ursolic acid induces Bax-dependent apoptosis through the caspase-3 pathway in endometrial cancer SNG-II cells. Oncol. Rep. 13, 51–57.

Altznauer, F., Conus, S., Cavalli, A., Folkers, G., Simon, H.U., 2004. Calpain-1 regulates Bax and subsequent Smac-dependent caspase-3 activation in neutrophil apoptosis. J. Biol. Chem. 279, 5947–5957.

Asaruddin, M.R., Honda, G., Tsubouchi, A., Nakajima-Shimada, J., Aoki, T., Kiuchi, F., 2003. Trypanocidal constituents from *Michelia alba*. Nat. Med. 57, 61–63.

Chen, C.H., Lo, W.L., Liu, Y.C., Chen, C.Y., 2006. Chemical and cytotoxic constituents from the leaves of *Cinnamomum kotoense*. J. Nat. Prod. 69, 927–933.

Chen, C.Y., Liu, T.Z., Liu, Y.W., Tseng, W.C., Liu, R.H., Lu, F.J., Lin, Y.S., Chen, C.H., 2007. 6-Shogaol (alkanone from Ginger) induces apoptotic cell death of human hepatoma p53 mutant Mahlavu subline via an oxidative stress-mediated caspase-dependent mechanism. J. Agric. Food Chem. 55, 948–954.

Cheng, J., Cui, R., Chen, C.H., Du, J., 2007. Oxidized low-density lipoprotein stimulates p53-dependent activation of proapoptotic Bax leading to apoptosis of differentiated endothelial progenitor cells. Endocrinology 148, 2085–2094.

Chipuk, J.E., Kuwana, T., Bouchier-Hayes, L., Droin, N.M., Newmeyer, D.D., Schuler, M., Green, D.R., 2004. Direct activation of Bax by p53 mediates mitochondrial membrane permeabilization and apoptosis. Science 303, 1010–1014.

Chulia, S., Ivorra, M.D., Cave, A., Cortes, D., Noguera, M.A., D'Ocon, M.P., 1995. Relaxant activity of three aporphine alkaloids from *Annona cherimolia* on isolated aorta of rat. J. Pharm. Pharmacol. 47, 647–650.

Hsieh, T.J., Liu, T.Z., Chia, Y.C., Chern, C.L., Tsao, D.A., Lu, F.J., Syu, Y.H., Hsieh, P.Y., Hu, H.S., Chang, T.T., Chen, C.H., 2005. Liriodenine inhibits the proliferation of human hepatoma cell lines by blocking cell cycle progression and nitric oxide-mediated activation of p53 expression. Food Chem. Toxicol. 43, 1117–1126.

Hsieh, T.J., Liu, T.Z., Lu, F.J., Hsieh, P.Y., Chen, C.H., 2006. Actinodaphnine induces apoptosis through increased nitric oxide, reactive oxygen species and down-regulation of NF-κB signaling in human hepatoma Mahlavu cells. Food Chem. Toxicol. 44, 344–354.

Jia, Z., Misra, H.P., 2007. Reactive oxygen species in *in vitro* pesticide-induced neuronal cell (SH-SY5Y) cytotoxicity: role of NFkappaB and caspase-3. Free Radical Biol. Med. 42, 288–298.

Lucke, J.F., 1996. Student's *t* test and the Glasgow Coma Scale. Ann. Emerg. Med. 28, 408–413.

Martinez, L.A., Rios, J.L., Paya, M., Alcaraz, M.J., 1992. Inhibition of nonenzymic lipid peroxidation by benzylisoquinoline alkaloids. Free Radical Biol. Med. 12, 287–292.

Mitsunaga, M., Tsubota, A., Nariai, K., Namiki, Y., Sumi, M., Yoshikawa, T., Fujise, K., 2007. Early apoptosis and cell death induced by ATX-S10Na (II)-mediated photodynamic therapy are Bax- and p53-dependent in human colon cancer cells. World J. Gastroenterol. 13, 692–698.

Paulo, M.Q., Barbosa-Filho, J.M., Lima, E.O., Maia, R.F., Barbosa, R.C., Kaplan, M.A., 1992. Antimicrobial activity of benzylisoquinoline alkaloids from *Annona salzmanii D.C.*. J. Ethnopharmacol. 36, 39–41.

Protais, P., Arbaoui, J., Bakkali, E.H., Bermejo, A., Cortes, D., 1995. Effects of various isoquinoline alkaloids on in vitro ^{3}H-dopamine uptake by rat striatal synaptosomes. J. Nat. Prod. 58, 1475–1484.

Raffo, A.J., Kim, A.L., Fine, R.L., 2000. Formation of nuclear Bax/p53 complexes is associated with chemotherapy induced apoptosis. Oncogene 19, 6216–6228.

Sharma, V., Joseph, C., Ghosh, S., Agarwal, A., Mishra, MK., Sen, E., 2007. Kaempferol induces apoptosis in glioblastoma cells through oxidative stress. Mol. Cancer Ther. 6, 2544–2553.

Syed, Meeran M., Suchitra, Katiyar, Santosh, Katiyar K., 2008. Berberine-induced apoptosis in human prostate cancer cells is initiated by reactive oxygen species generation. Toxicol. Appl. Pharmacol. 229, 30–43.

Tsai, I.L., Liou, Y.F., Lu, S.T., 1989. Screening of isoquinoline alkaloids and their derivatives for antibacterial and antifungal activities. Gaoxiong Yi Xue Ke Xue Za Zhi 5, 132–145.

Ubeda, A., Montesinos, C., Paya, M., Alcaraz, M.J., 1993. Iron-reducing and free-radical-scavenging properties of apomorphine and some related benzylisoquinolines. Free Radical Biol. Med. 15, 159–167.

Valiente, M., D'Ocon, P., Noguera, M.A., Cassels, B.K., Lugnier, C., Ivorra, M.D., 2004. Vascular activity of (−)-anonaine, (−)-roemerine and (−)-pukateine, three natural 6a(R)-1,2-methylenedioxyaporphines with different affinities for alpha1-adrenoceptor subtypes. Planta Med. 70, 603–609.

Villar, A., Mares, M., Rios, J.L., Canton, E., Gobernado, M., 1987. Antimicrobial activity of benzylisoquinoline alkaloids. Pharmazie 42, 248–250.

Wang, Y., Perchellet, E.M., Ward, M.M., Lou, K., Zhao, H., Battina, S.K., Wiredu, B., Hua, D.H., Perchellet, J.P., 2006. Antitumor triptycene analogs induce a rapid collapse of mitochondrial transmembrane potential in HL-60 cells and isolated mitochondria. Int. J. Oncol. 28, 161–172.